

Elasticity, stability, and ideal strength of β -SiC in plane-wave-based *ab initio* calculations

Weixue Li and Tzuchiang Wang

Laboratory for Nonlinear Mechanics of Continuous Media (LNM), Institute of Mechanics, Chinese Academy of Sciences, Beijing, 100080, China

(Received 9 March 1998; revised manuscript received 9 July 1998)

On the basis of the pseudopotential plane-wave method and the local-density-functional theory, this paper studies energetics, stress-strain relation, stability, and ideal strength of β -SiC under various loading modes, where uniform uniaxial extension and tension and biaxial proportional extension are considered along directions [001] and [111]. The lattice constant, elastic constants, and moduli of equilibrium state are calculated and the results agree well with the experimental data. As the four Si-C bonds along directions [111], $[\bar{1}\bar{1}1]$, $[11\bar{1}]$, and $[1\bar{1}\bar{1}]$ are not the same under the loading along [111], internal relaxation and the corresponding internal displacements must be considered. We find that, at the beginning of loading, the effect of internal displacement through the shuffle and glide plane diminishes the difference among the four Si-C bonds lengths, but will increase the difference at the subsequent loading, which will result in a crack nucleated on the {111} shuffle plane and a subsequently cleavage fracture. Thus the corresponding theoretical strength is 50.8 GPa, which agrees well with the recent experiment value, 53.4 GPa. However, with the loading along [001], internal relaxation is not important for tetragonal symmetry. Elastic constants during the uniaxial tension along [001] are calculated. Based on the stability analysis with stiffness coefficients, we find that the spinodal and Born instabilities are triggered almost at the same strain, which agrees with the previous molecular-dynamics simulation. During biaxial proportional extension, stress and strength vary proportionally with the biaxial loading ratio at the same longitudinal strain. [S0163-1829(99)02406-6]

I. INTRODUCTION

Investigation of stability and ideal strength of materials is always an attractive issue¹⁻⁹ due to the following facts: (1) Stability of materials is very important in elasticity theory, which is related with structural responses in solids, ranging from polymorphism, amorphization, and melting to fracture.¹⁰⁻¹³ (2) The ideal strength of a perfect crystal represents an upper bound to the actual strength of crystalline materials. (3) The technology makes it possible to manufacture finer and finer filament, whose strength will approach the theoretical limit. However, even for the best whisker materials^{14,15} the realistic strength is still far below the predicted theoretical values.

Recent developments of experimental technology create new opportunities of producing very fine nanorods (NR's) and nanotubes (NT's),¹⁶⁻²⁰ and the possibility of measuring their elasticity constants, strength, and toughness.^{21,22} The typical measured diameter of NR's is 20-30 nm, which can be considered free of any defects and with the ideal strength. Wong *et al.*²² measured Young's modulus and the bending strength of silicon carbon (SiC) NR's in a recent experiment. It is worth mentioning that micrometer-scale SiC whisker is widely used to strengthen composite materials. Thus, it is necessary to have a clear understanding of the stiffness, stress-strain relation, stability, and strength of these nano-sized NR's from the experimental view as well as from the theoretical point of view.

As is well known, people are used to study the ideal strength of materials with various models and empirical potentials. Polanyi²³ and Orowan²⁴ used a model in terms of surface energy, interplanar space, and an appropriate Young's modulus to investigate the ideal strength. Frenkel¹ estimated ideal shear strength τ_{max} of a solid subjected to

deformation of a simple shear mode. However, oversimplified functions of stress-strain were adopted in those methods and the functional forms for different materials were somehow arbitrary. On the basis of stability criteria, Milstein and co-worker³⁻⁵ investigated the theoretical strength of bcc Fe and fcc Ni and Cu with the Morse potential. The ideal strength is identified with the loss or exchange of stability. This method helps greatly the investigation of strength and reveals a variety of interesting and surprising behaviors of materials;²⁵⁻²⁸ however, the interatomic potential they used and obtained by fitting properties of equilibrium state is inappropriate for use in the investigation of the stability and strength of materials, which are essentially far from being in the equilibrium state. On the other hand, the density-functional theory (DFT),²⁹ with only the input of atomic position and charge number, can be used to determine many structural and dynamic properties of materials under various conditions, including those that are far from being in the equilibrium state.

Through a series of comprehensive theoretical and computational studies, Hill and Milstein³¹⁻³³ have shown that positive definiteness of internal energy is coordinate dependent and the stability domain depends on the choices of strain measures, while Born criteria³⁰ are valid only under the zero load. Based on this idea, Wang and co-workers^{11,12} analyzed the onset of instabilities in homogeneous lattice under critical loading and showed that response of the lattice is no longer a purely intrinsic property of materials and depends on the applied load. Starting with these theories, Li and Wang³⁴ have recently analyzed the stability and branching of aluminum under various loading modes according to first-principles calculations.

Heine and co-workers^{35,36} gave a very extensive set of

first-principles pseudopotential calculations on the ploy types in SiC. However, they gave only the bulk modulus. Lambrecht *et al.*³⁷ made a detailed investigation on the elastic constants and modulus of β -SiC with the full-potential-linear-muffin-tin-orbital (FP-LMTO) method. In their investigations, the strength of β -SiC was obtained approximately by Orowan formula. The structural properties of β -SiC (ploy type 3C) had been also investigated by the various semiempirical models, e.g., semiempirical force model,³⁸ semiempirical interatomic potential,^{39,40} and tight-binding approximation.^{41,42} Modifying the Tersoff potential,³⁹ Tang and Yip⁴³ investigated the lattice instability in β -SiC and simulated the process of brittle fracture under hydrostatic tension based on the Hill and Milstein stability theory. The instability mode is the spinodal instability and decohesion occurs as spontaneous nucleation of cracking on the {111} shuffle planes.

In the present paper, we study the energetics, the elastic constants, the stress-strain relation, stability, and the ideal strength of β -SiC with the density-functional theory. We consider several loading modes, uniaxial extension, and uniaxial tension along [001] and [111] directions, and biaxial proportional extension along [001] and [010]. The deformation is homogeneous and elastic and the strain can be large. The stress-strain relations are calculated, and the ideal strength is obtained according to the stability criteria. Owing to the nonequivalence of the four Si-C bonds under the loading along [111], the internal relaxation must be considered and the internal displacements be calculated. With the internal displacements, we discuss the effect of the relaxation and failure modes. The stability theory of Hill and Milstein³¹⁻³³ and Wang *et al.*¹² are used to discuss branching and the strength of β -SiC under the loading along [001].

The present paper is organized as follows. The calculation model is presented in Sec. II, where we show the formulation of stress, elastic stiffness coefficients, and stability criteria, especially the three loading modes with the selection of supercell and the numerical precision illustrated at the end of this section. The benchmark, including equilibrium properties and elastic constants, are given in Sec. III. The loading along [111] direction is presented in Sec. IV, and biaxial proportional extension is investigated in Sec. V. In Sec. VI, we discuss uniaxial extension and tension along [001] direction. Summary and conclusion are given in Sec. VII.

II. FORMULATION

Consider an unstressed and unstrained configuration, denoted as \mathbf{X}_0 . It undergoes homogeneous deformation under a uniform applied force, and changes from \mathbf{X}_0 to $\mathbf{X}=\mathbf{J}\mathbf{X}_0$, where \mathbf{J} is the deformation gradient or the Jacobian matrix. The associated Lagrangian strain tensor \mathbf{E} is

$$\mathbf{E}=\frac{1}{2}(\mathbf{J}^T\mathbf{J}-\mathbf{I}), \quad (1)$$

where T is transpose. The physical strain is

$$\mathbf{e}=\mathbf{J}-\mathbf{I}. \quad (2)$$

For the present deformation, the internal energy U is a rotational invariant and therefore only a function of \mathbf{E} . The second Ploa-Kirchhoff stress tensor \mathbf{T} (Ref. 44) is defined as

$$T_{ij}=\frac{1}{V_0}\frac{\partial U}{\partial E_{ij}}. \quad (3)$$

It is related to Cauchy stress, i.e., the true stress σ_{kl} by the following equation:

$$T_{ij}=\mathbf{det}|\mathbf{J}|J_{ik}^{-1}J_{jl}^{-1}\sigma_{kl}, \quad (4)$$

where $\mathbf{det}|\mathbf{J}|$ is the ratio V/V_0 . With the Cauchy stress, the applied force can be obtained by multiplying the current transverse area.

At strained state \mathbf{X} , the elastic constants are determined through the following equation:

$$C_{ijkl}(X)=\frac{1}{V(X)}\left(\frac{\partial^2 U}{\partial E'_{ij}\partial E'_{kl}}\Bigg|_{E'=0}\right), \quad (5)$$

where \mathbf{E}' is Lagrangian strain around the state \mathbf{X} . These elastic constants are rotational invariant and symmetric with interchange of indices $i\leftrightarrow j$, $k\leftrightarrow l$, and $(ij)\leftrightarrow(kl)$, which are often expressed in the condensed Voigt notation.

To analyze the stability, the elastic stiffness coefficient \mathbf{B} (Ref. 12) is introduced as follows:

$$B_{ijkl}=C_{ijkl}+\frac{1}{2}(\delta_{ik}\sigma_{jl}+\delta_{jk}\sigma_{il}+\delta_{il}\sigma_{jk}+\delta_{jl}\sigma_{ik}-2\delta_{kl}\sigma_{ij}). \quad (6)$$

From this definition, we can see that \mathbf{B} does not possess $(ij)\leftrightarrow(kl)$ symmetry generally. The system may be unstable when

$$\mathbf{det}|\mathbf{B}|=0 \quad (7)$$

for the first time.

The following loading modes are considered: (i) uniaxial extension,

$$e_{ij}=e\delta_{i3}\delta_{j3}, \quad i,j=1,2,3; \quad (8)$$

(ii) uniaxial tension,

$$\sigma_{ij}=\sigma\delta_{i3}\delta_{j3}, \quad i,j=1,2,3. \quad (9)$$

For a given longitudinal strain, let the transverse lattice contract or dilate to make the total-energy approach minimum, which corresponds zero stress (traction) on lateral faces. For crystal symmetry, the transverse contraction is the same at two perpendicular transverse directions, so

$$e_{11}=e_{22}=-\lambda e_{33}. \quad (10)$$

(iii) biaxial proportional extension is a third mode, where

$$e_{22}=\alpha e_{33}\neq 0, \quad e_{ij}=0, \quad \text{others}. \quad (11)$$

The total-energy calculations are carried out with an *ab initio* pseudopotential plane-wave program package FHI96MD.⁴⁵ By means of the mechanism of Hamann⁴⁶ and Troullier and Martins,⁴⁷ the soft first-principles pseudopotential^{48,49} is generated, where the local-density approximation (LDA) with the exchange and correlation energy functional developed by Perdew and Zunger⁵⁰ is used. Two supercells are designed in our calculations: one is the eight-atom supercell for the equilibrium properties, the loading along [001], and biaxial extension along [010] and [001]. The other one is the six-atom supercell for the loading along

TABLE I. Equilibrium and elastic modulus of β -SiC. PP-PW, present pseudopotential plane-wave calculations; FP-LMTO, Lambrecht *et al.* (Ref. 37); CKH, Churcher, Kunc, and Heine (Ref. 35); Tolpygo (Ref. 38); Tersoff (Ref. 39); Expt., experimental values as indicated by footnotes. The length unit is the bohr radius and the modulus is GPa; the anisotropy $A = 2C_{44}/(C_{11} - C_{12})$.

	PP-PW	FP-LMTO	CKH	Tolpygo	Tersoff	Expt.
a_0	8.166	8.154	8.145		8.164	8.238 ^a
B_0	225	223	224	211	220	225 ^b
C_{11}	405	420		352.3	420	390 ^c
C_{12}	135	126		140	120	142 ^c
C_{44}	254(270)	287		232	260	256 ^c
A	1.88	1.95		2.20	1.73	2.00 ^c
E_{111}	558	603		511	560	581($\pm 10\%$) ^d 610 ^e
E_{100}	338	362		272	367	
E_R	441	476		378	462	
E_V	474	516		424	488	
E_a	458	496		401	475	448 ^b
G_R	188	208		157	201	
G_V	206	231		182	216	
G_a	197	219		169	208.5	192 ^b
ν_a	0.173	0.146		0.201	0.150	0.168 ^b

^aReference 53.

^bCarnahan (Ref. 54).

^cObtained from sound velocities (Ref. 55).

^dExperimental values from whisker (Ref. 15).

^eExperimental values from nanorods (Ref. 22).

[111]; in this case, the stacking consequence is Si-C-Si-C-Si-C. There exist two types of {111} plane, between Si and C atoms, corresponding to the well-known glide and shuffle planes. The glide plane cuts three Si-C bonds out of four, and the shuffle plane cuts the remaining Si-C bond. For numerical differential feature of stress and elastic constants, the precision must be considered carefully. The size of carbon atom is so small that a high cut-off energy is required. Our test shows that $E_{cut} = 80$ Ry has also given excellent results. The k -space mesh is $6 \times 6 \times 6$ for the eight-atom supercell and $8 \times 8 \times 4$ for the six-atom supercell in order to keep the same precision.

III. EQUILIBRIUM PROPERTIES

As the benchmark, we have calculated the lattice constant, elastic constants, and moduli of β -SiC of equilibrium. For symmetry of β -SiC (zinc-blende structure), there exist three independent elastic constants, i.e., C_{11}, C_{12}, C_{44} . The total energy of β -SiC is calculated under the applied hydrostatic, uniaxial deformation, and trigonal strain. Owing to the lattice feature of zinc-blende structure, which includes two fcc lattices with a relative displacement along [111], the symmetry of center inversion is lost. Four Si-C bonds along directions [111], $[1\bar{1}1]$, $[11\bar{1}]$, and $[\bar{1}11]$ are not equivalent under the case of trigonal strain. The internal atomic position must be fully relaxed, and the internal displacement,⁵¹ which refers to the relative displacement of two sublattices beside the displacement from the macroscopic strain, will take place. Our results are presented in Table I. From this table, we find our results agree well with the experimental data and the previous first-principles and semiempirical calculations. The value

of C_{44} without relaxation, 270 GPa, is already in good agreement with the experimental data and better than other theoretical calculations. The relaxed value, 254 GPa, is almost the same as the experiment value. Value of the anisotropy A is also satisfactory.

Based on the representation surface,⁵² the moduli along a certain direction can be obtained. Young's modulus along directions [111] and [001] is 554 GPa and 338 GPa, respectively. Lambrecht *et al.*³⁷ obtained 603 GPa and 362 GPa. Petrovic *et al.*¹⁵ measured Young's modulus of β -SiC whisker, with an averaged value of 578 GPa with $\pm 10\%$ scattering. Applying the equation of the cantilever beam, Wong *et al.*²² measured Young's modulus of [111]-oriented SiC nanorod, which are 610 GPa and 660 GPa, corresponding to the 23.0-nm diameter and 21.5-nm diameter SiC NR's. The agreement is good.

With orientation averages, the moduli of isotropic materials can be obtained. Two average methods, namely, Reuss averages⁵⁶ (E_R and G_R) and Voigt averages⁵⁷ (E_V and G_V), are adopted. According to the theory of Hill,⁵⁸ the physical averages, here denoted by subscript a , are the intermediate between the Reuss and Voigt averages. With these considerations, Young's modulus and shear modulus of isotropic β -SiC are given as follows:

$$E_a \approx 448 \text{ GPa} \pm 2.2\%,$$

$$G_a \approx 192 \text{ GPa} \pm 2.6\%.$$

Compared with the previous first-principles³⁷ and semiempirical^{38,39} calculations, our results agree better with the experimental values. These results confirm the conclusion of Lambrecht: the random orientation hypothesis applies

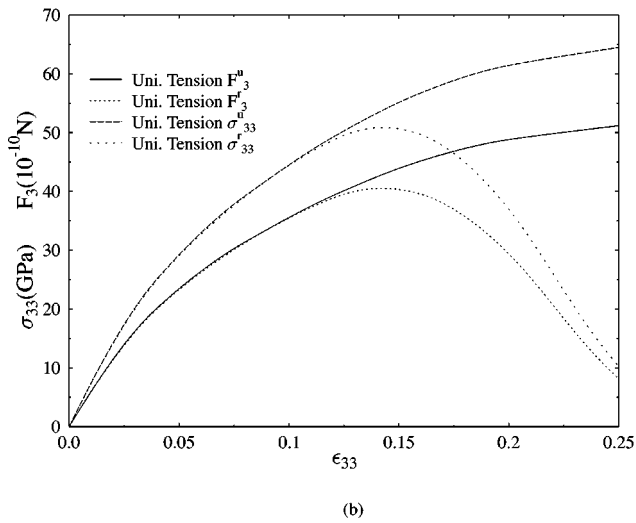
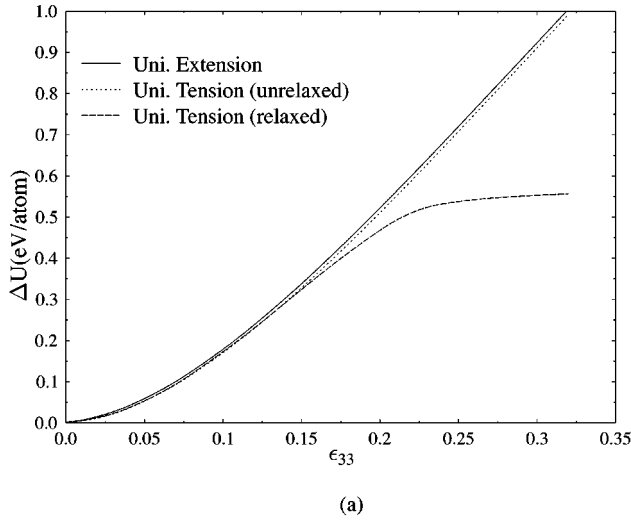


FIG. 1. (a) The calculated strain energy under the uniaxial extension and uniaxial tension with or without internal relaxation. (b) Applied force and stress under uniaxial tension with or without relaxation.

well to the ceramic samples. The average Poisson ratio ν_a , 0.17, is close to the experimental value. The small Poisson ratio of β -SiC, as compared with other materials, e.g., aluminum 0.347, demonstrates its high stiffness.

IV. LOADING ALONG DIRECTION [111]

In this loading direction, two loading modes are investigated: uniaxial extension and uniaxial tension. At the latter case, the transverse lattices contract in order to approach the energy minimum. With regard to the loss of symmetry of center inversion, the four Si-C bonds along directions [111], $[1\bar{1}1]$, $[11\bar{1}]$, and $[\bar{1}11]$, are not equivalent under [111] loading. The internal relaxation and lateral contraction must be considered. In our calculations, by using the lattice constant at room temperature, the internal relaxation is carried out after the transverse strains are obtained. The length of Si-C bond is 3.5673 (bohrs) under zero loading. As the loading is along [111] direction, the variation of bond length along the [111] direction will be more significant than that of the other three bonds. Figure 1 shows the energy, stress, and

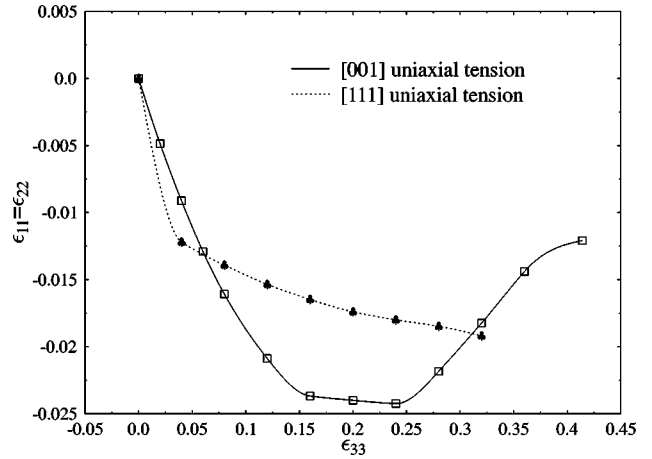


FIG. 2. The transverse strain of uniaxial tension along directions [001] and [111].

force under uniaxial extension and uniaxial tension with or without internal displacement. (Without other statement, the strain, force, and stress, given in the figures, are the physical strain, applied force, and Cauchy stress.) The corresponding transverse strain and internal displacement are given in Fig. 2 and Fig. 3.

At the beginning of loading, as compared with the corresponding Si-C bond length without the internal relaxation, the difference among the four Si-C bond lengths is small, and no marked effect of relaxation and internal displacement through both the shuffle and glide plane is shown. This phenomenon, shown in Fig. 1, is obvious for β -SiC, a kind of high stiffness and low Poisson ratio covalent material. The strain energy curves of the three loading modes, i.e., uniaxial extension and uniaxial tension with or without internal relaxation, are almost the same. Despite the fact that the stress and force of uniaxial tension is smaller than the uniaxial extension for the relaxation, they are still similar in these loading modes. Based on Kleinman's⁵⁹ discussion on silicon with [111] strain, the internal strain tends to keep the bond length along the four unchanged unequivalent [111] directions. In our calculations, the internal displacement of atom along [111] direction, which is through the shuffle plane, is nega-

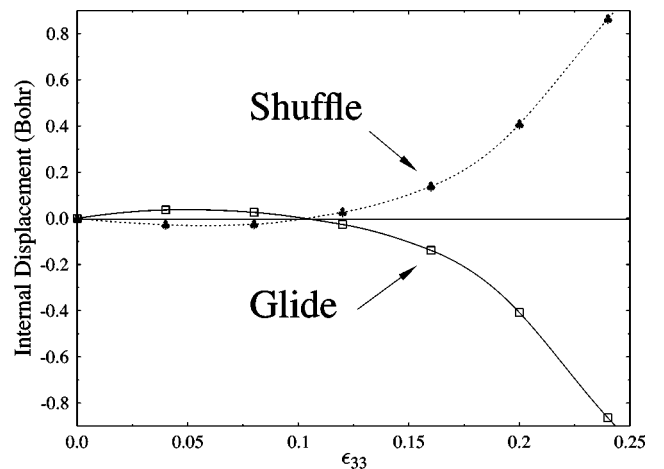


FIG. 3. The internal displacement through shuffle and glide plane under [111] uniaxial tension. The club is for the shuffle plane and the square is for the glide plane.

TABLE II. The Young's modulus and strength compared to other theoretical calculations and experiments. Here, ts, bs, and cs mean the tensile strength, the bending strength, and the cleavage strength. The unit is GPa.

	E	σ_{ts}	E^a	σ_{ts}^a	σ_{cs}^b	E^c	σ_{bs}^c	E^d	σ_{ts}^d
[111]	558	50.4(0.144)	603	30	46.3	610	53.4	$580 \pm 10\%$	23.74
[001]	338	101(0.37)	362						

^aFrom FP-LMTO and Orwan expression (Ref. 37).

^bFrom Orwan expression (Ref. 60).

^cExperimental values from nanorods (Ref. 22).

^dExperimental values from whiskers (Ref. 15).

tive, and that of the remaining three Si-C bonds along the $[1\bar{1}1]$, $[11\bar{1}]$, and $[\bar{1}11]$ directions, through the glide plane, is positive. This means that the effect of relaxation always tends to diminish the difference of four Si-C bond lengths. With the increase of the longitudinal strain, the internal displacement through the shuffle plane becomes positive from negative, and that through the glide plane moves from positive to negative while approaching zero at the same point ($e_z = 0.105$). The internal displacements for the two cases have the same magnitude but with the opposite sign. The details can be found in Fig. 3. During the whole uniaxial tension, the magnitude of transverse strain increases monotonically.

With further increase of the longitudinal strain, the strain energy of uniaxial extension and of uniaxial tension without internal displacement still have approximately the same value. However, both the internal displacements through the shuffle plane and the glide plane change their signs (the symmetry still holds). The uniaxial tension curve with internal relaxation softens quickly and the shape of tensile curve changes dramatically. An energy plateau presents, and material becomes unstable. On the basis of the stress curve, the maximum stress of uniaxial tension with internal relaxation, namely, the theoretical strength σ_{th} , is obtained and equal to 50.8 GPa. The corresponding critical macroscopic strain and internal displacement is 0.144 and 0.082 (bohr), the Si-C bond length along [111] is 4.163 (bohrs). With the modified Tersoff potential, Tang and Yip⁴³ analyzed the brittle fracture of β -SiC under hydrostatic tension by molecular dynamics. They found that the mode of instability of β -SiC was the spinodal instability and the corresponding critical strain and pressure were 0.153 and 37.0 GPa. Therefore, both the first-principles and empirical potential calculations gave a similar critical bond length of β -SiC along [111].

Our result agrees well with the experimental value, given by Wong *et al.*,²² 53.4 GPa, obtained for the [111]-oriented SiC nanorod. This agreement also means that no other branching and instability modes exist during the uniaxial loading before it reaches the inflexion of an energy-strain curve. It is worthwhile pointing out that the experimental strength measured is the bending strength. The tensile and bending strengths are comparable to β -SiC whisker^{8,15} and are also expected to be similar to the β -SiC nanorod.²² Petrovic *et al.*¹⁵ measured the tensile strength of β -SiC whisker and their result is 23.74 GPa, which is far smaller than our theoretical calculation and Wong's experiment values for defects. Lambrecht *et al.*³⁷ calculated the tensile strength by Orwan expression with [111] surface energy, and the result

is 30 GPa. With the similar formula, Op Het Veld and Veldkamp⁶⁰ obtained the theoretical cleavage strength 46.3 GPa, which is close to ours. The detailed comparison can be found in Table II.

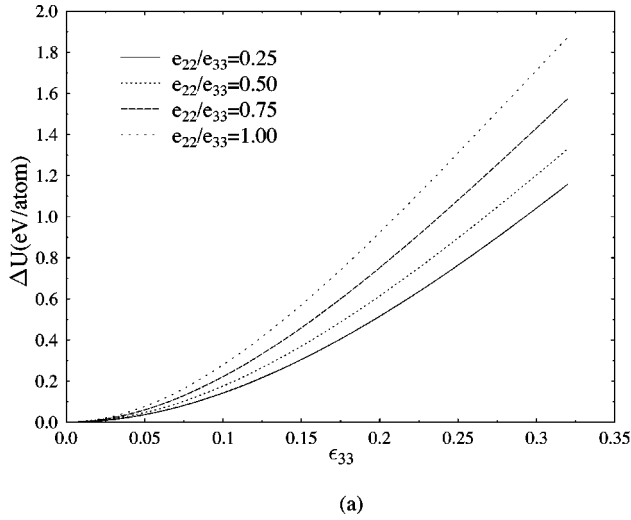
After $e_z > 0.105$, the internal displacement through the shuffle plane becomes positive, and that through the glide plane becomes negative. The distance between the atom through the shuffle plane along [111] increases, and that through the glide plane decreases, and a crack nucleates on the {111} shuffle plane. The internal displacements through the shuffle and glide plane at the critical strain are, respectively, 0.082 and -0.082 . With further increase of the longitudinal strain, the internal displacements of the shuffle and glide planes also increase quickly. This positive and negative increase of internal displacements of shuffle and glide planes will result in a dramatic cleavage on the {111} shuffle plane and the mixing of Si and C atoms through the glide plane. The cleavage on {111} shuffle plane can be partly attributed to the lower surface energy than that of the {111} glide plane.^{31,43,61} These results agree well with the previous molecular-dynamics simulation.⁴³

V. BIAXIAL PROPORTIONAL EXTENSION

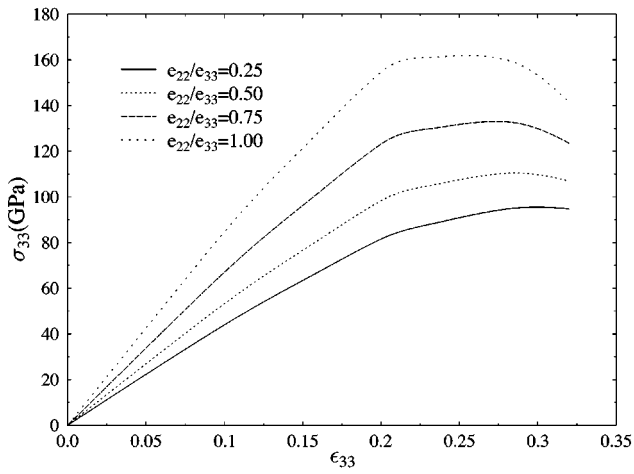
To consider only the biaxial proportional extension, this section deals with the extension along directions [010] and [001], and not the internal atomic and volume relaxation. The strain ratio between [010] and [001] is 0.25, 0.5, 0.75, and 1. The results are shown in Fig. 4. With the increase of the ratio, the energy, stress, and maximum stress will increase at the same longitudinal strain accordingly. However, the critical strain is similar for different proportional loading modes.

VI. LOADING ALONG DIRECTION [001]

In this section, we consider the uniaxial extension and uniaxial tension along direction [001]. The reference state is the state with the theoretical lattice constant. Symmetry of crystal under this loading mode is tetragonal. Unlike the loading along [111], the deformation of the four Si-C bonds in this loading mode is the same and the four bonds are equivalent. There will not be any internal displacements and the internal relaxation can be neglected during the loading. We have made calculations at several strains with or without internal relaxation and found that the value of transverse strain at a specific longitudinal strain is the same. Our results are given in Figs. 2 and 5.



(a)

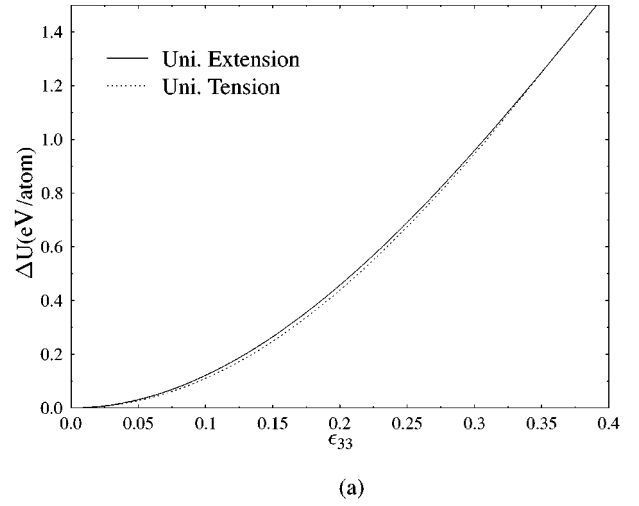


(b)

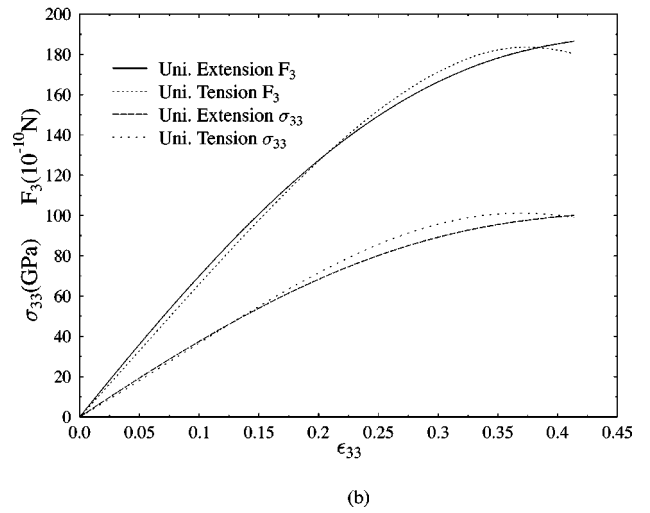
FIG. 4. The calculated strain energy (a) and applied stress (b) during biaxial proportional extension with difference ratio along [010] (e_{22}) and [001] (e_{33}) directions.

From Fig. 5(a), we can see that both of the strain energy for uniaxial extension and tension increase with the increase of the longitudinal strain. The strain energy of uniaxial extension is always larger than that of the uniaxial tension, as is expected. However, the energy difference between two loading modes is small, the same as with the [111] loading. At a larger strain, the energy difference becomes even smaller. The applied force and stress of uniaxial tension are lower than those of the uniaxial extension for the triaxial stress state at the beginning and higher than them at the subsequent loading (this phenomenon will be explained later). Just like Fig. 5(a), the difference of applied force and stress between these two loading modes is not significant.

In order to obtain the ideal strength and analyze the stability under uniaxial tension, we calculate the elastic constants and derive the stability criteria based on the stiffness coefficients. With the tetragonal symmetry, the number of independent elastic constants is reduced to six: C_{33} , C_{12} , $C_{13}=C_{23}$, $C_{11}=C_{22}$, $C_{44}=C_{55}$, and C_{66} ; all the other C_{ij} are equal to zero. With Eqs. (6), (7), and (9), we write the stability criteria as follows:



(a)



(b)

FIG. 5. The calculated strain energy (a), applied force and stress (b) of uniaxial extension and uniaxial tension along direction [001].

$$(C_{33} + \sigma)(C_{11} + C_{12}) - 2C_{13}(C_{13} - \sigma) \geq 0, \quad (12)$$

$$C_{11} - C_{12} \geq 0, \quad (13)$$

$$C_{44} + \frac{1}{2}\sigma \geq 0, \quad (14)$$

$$C_{66} \geq 0. \quad (15)$$

The first one involves the vanishing of bulk modulus, and is referred to as spinodal instability. The second instability involves symmetry breaking (bifurcation) with the volume conservation; it may be identified as the tetragonal shear breaking and referred to as Born instability. The third and fourth are two distinct shear deformation instabilities. Six strains are designed to calculate the independent elastic constants and are given as follows:

$$e_{11} = e_{22} = \delta, \quad e_{ij} = 0, \quad i, j = 1, 2, 3,$$

$$e_{11} = -e_{22} = \delta, \quad e_{ij} = 0, \quad i, j = 1, 2, 3,$$

$$e_{11} = e_{33} = \delta, \quad e_{ij} = 0, \quad i, j = 1, 2, 3,$$

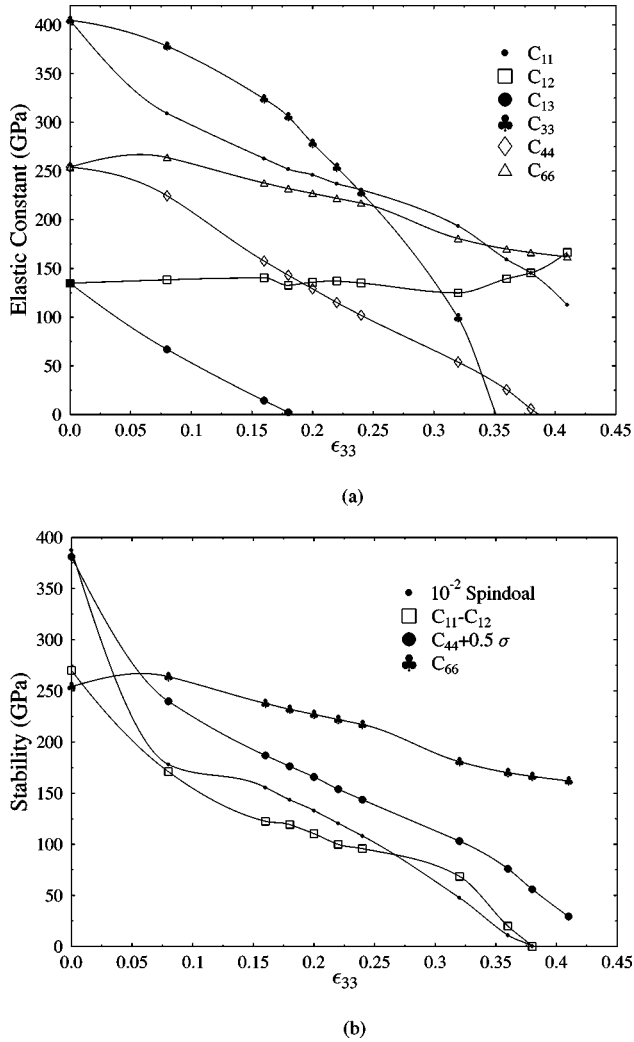


FIG. 6. The calculated elastic constants (a) and stability (b) during uniaxial tension along direction [001].

$$e_{11} = -e_{33} = \delta, \quad e_{ij} = 0, \quad i, j = 1, 2, 3,$$

$$e_{12} = e_{21} = \delta, \quad e_{ij} = 0, \quad i, j = 1, 2, 3,$$

$$e_{23} = e_{32} = \delta, \quad e_{ij} = 0, \quad i, j = 1, 2, 3.$$

In each case, the domain of strain is $[0, 0.02]$. The results are shown in Fig. 6.

During uniaxial tension, the variation of mechanical properties on the transverse section is comparatively small, and the corresponding elastic constants, i.e., C_{11} , C_{12} , C_{66} , keep positive, as shown in Fig. 6(a). However, the elastic constants related to longitudinal strain change dramatically and even become negative at large strain, e.g., $C_{13} \leq 0$ when $e_{33} \geq 0.184$, $C_{33} \leq 0$ when $e_{33} \geq 0.352$. Because $C_{13} \leq 0$ leads to negative Poisson ratio, the transverse section will expand with the increase of the longitudinal strain. This phenomenon is also shown in Fig. 2; the transverse strain varies e_{11} proportionally with e_{33} when $e_{33} \geq 0.20$. Negative Poisson ratio had also been investigated by Milstein and co-workers.^{3,4,26,62} However, in their papers, negative Poisson ratio only occurs at branching or unstable points, and the materials investigated are monatomic metal materials Fe and

Ni. In the present calculations, it is surprising that β -SiC, a nonmetal and two-component crystal, is still stable at this negative Poisson ratio, shown in Fig. 6(b). The same result is obtained when calculations with internal atomic relaxation are implemented. This phenomenon must be related with the bond nature of β -SiC. The charge transfer⁶³ and ionic component⁶⁴ of β -SiC will affect the mechanical response. The detailed analysis of electric structure should be carried out and further investigation is necessary. The lattice transverse expansion leads to much quicker increase of the force and stress of uniaxial tension than that of uniaxial extension and the values of the previous force and stress will be higher than those of uniaxial extension at a large strain.

On the basis of the stability criteria, we have found that the spinodal and Born instabilities are triggered almost at the same strain 0.37 with the transverse strain -0.0137 . The corresponding strength, 101.3 GPa, which is almost twice of that for [111]-oriented SiC nanorod, 53.4 GPa (Ref. 22) for its smaller interplanar distance, is obtained. At this critical strain, the elongation strain along [111] direction is 0.129, comparable with the critical strain 0.144 under uniaxial loading along [111]. Tang and Yip⁴³ investigated the instability of β -SiC under hydrostatic tension with stiffness coefficient, and found that failure mode of β -SiC is spinodal instability. This was proved by their molecular-dynamics simulations, and the nucleation of cracking on the $\{111\}$ plane and decohesion were revealed. They also showed that a shear instability is triggered by the spinodal instability. All of these results are same with our first-principles calculations.

VII. SUMMARY AND CONCLUSION

On the basis of the DFT total-energy calculation and stability theory, we give a detailed investigation of the mechanical properties of a two-atomic constituent material β -SiC: energetics, elasticity, stress-strain relations, stability, and strength under different loading modes and directions. The results are satisfactory.

Owing to the unequivalence of the four Si-C bonds under the uniaxial tension along [111], the relaxation must be implemented and internal displacements calculated. The internal displacements along the [111] direction and the other three directions, namely, $[\bar{1}11]$, $[1\bar{1}1]$, and $[1\bar{1}\bar{1}]$ have the same magnitude but the opposite sign. At the beginning of loading, the effect of relaxation is not significant and tends to diminish the difference of the four Si-C bond lengths. However, it becomes important at the subsequent loading and results in a crack nucleated on the $\{111\}$ shuffle plane, while the Si atom and C atom through the glide plane approach each other. The failure in this loading modes is of cleavage fracture. These conclusions are consistent with the previous molecular-dynamics simulations. The theoretical strength obtained agrees well with the experimental data.

Under loading along [001], the four Si-C bonds are equivalent for the tetragonal symmetry and the relaxation can be neglected. The strain energy, applied force, and stress are similar despite two distinct loading modes, namely, uniaxial tension and extension. During the uniaxial loading along [001], the spinodal and Born instabilities are triggered almost at the same strain. Previous molecular-dynamics investigation revealed similar facts. Owing to the smaller in-

terplanar distance, the corresponding ideal strength, 101 GPa, which is much higher than the theoretical strength for the loading along [111] and the experimental data, is obtained; however, the Si-C bond length for loading along [001] and [111] at the critical strain is close. There exists some stable range when the Poisson ratio is negative, and these phenomena are related to the unique bond nature of β -SiC, a kind of nontypical covalent material, which permits charge transfer. A detailed analysis of electronic structure will be brought up for further investigation.

ACKNOWLEDGMENTS

This work was supported by the National Natural Science Foundation of China (Grant No. 19704100) and the National Natural Science Foundation of the Chinese Academy of Sciences (Grant No. KJ951-1-201). One of the authors W.X.L. wishes to thank Professor D.S. Wang for his helpful discussion and encouragement. Parts of the computations are done at the super-parallel computer of the Network Information Center of the Chinese Academy of Sciences. We are also grateful to Professor K. Wang for checking the manuscript.

- ¹J. Frenkel, *Z. Phys.* **37**, 572 (1926).
- ²A. Kelly, *Strong Solids*, 2nd ed. (Clarendon, Oxford, 1973).
- ³F. Milstein, *Phys. Rev. B* **3**, 1130 (1971).
- ⁴F. Milstein, *J. Appl. Phys.* **44**, 3833 (1973).
- ⁵F. Milstein and B. Farber, *Philos. Mag. A* **42**, 19 (1980).
- ⁶E. Esposito, A. E. Carlsson, D. D. Ling, H. Ehrenreich, and C. D. Gelatt, Jr., *Philos. Mag. A* **41**, 251 (1980).
- ⁷A. T. Paxton, P. Gumbsch, and M. Methfessel, *Philos. Mag. Lett.* **63**, 267 (1991).
- ⁸N. H. Macmillan, *J. Mater. Sci.* **7**, 239 (1972).
- ⁹M. Šob, L. G. Wang, and V. Vitek, *Mater. Sci. Eng., A* **234-236**, 1078 (1997); P. Šandera, J. Pokluda, L. G. Wang, and M. Šob, *ibid.* **234-236**, 370 (1997).
- ¹⁰F. Cleri, J. Wang, and S. Yip, *J. Appl. Phys.* **77**, 1449 (1995).
- ¹¹J. Wang, S. Yip, S. Phillpot, and D. Wolf, *Phys. Rev. Lett.* **77**, 4182 (1993).
- ¹²J. Wang, J. Li, S. Yip, S. Phillpot, and D. Wolf, *Phys. Rev. B* **52**, 12 627 (1995).
- ¹³K. Mizushima, S. Yip, and E. Kaxiras, *Phys. Rev. B* **50**, 14 952 (1994).
- ¹⁴R. L. Mehan and J. A. Herzog, in *Whisker Technology*, edited by A. P. Levitt (Wiley-Interscience, New York, 1970), pp. 157–196.
- ¹⁵J. J. Petrovic, J. V. Milewski, D. L. Rohr, and F. D. Gac, *J. Mater. Sci.* **20**, 1167 (1985); J. J. Petrovic and R. C. Hoover, *ibid.* **22**, 517 (1987); N. H. Macmillan, *ibid.* **7**, 239 (1972).
- ¹⁶T. W. Ebbesen and P. M. Ajayan, *Nature (London)* **358**, 220 (1995).
- ¹⁷D. T. Colbert *et al.*, *Science* **266**, 1218 (1994).
- ¹⁸T. Guo, P. Nikolaev, A. Thess, D. T. Colbert, and R. E. Smalley, *Chem. Phys. Lett.* **243**, 49 (1995); A. Thess *et al.*, *Science* **273**, 483 (1996).
- ¹⁹H. Dai, E. W. Wong, Y. Z. Lu, S. Fan, and C. M. Lieber, *Nature (London)* **375**, 769 (1995).
- ²⁰P. Yang and C. M. Lieber, *Science* **273**, 1836 (1996).
- ²¹H. Dai, E. W. Wong, and C. M. Lieber, *Science* **272**, 523 (1996).
- ²²E. W. Wong, P. E. Sheehan, and C. M. Lieber, *Science* **277**, 1971 (1997).
- ²³M. Polanyi, *Z. Phys.* **7**, 323 (1921).
- ²⁴E. Orowan, *Z. Kristallogr.* **89**, 327 (1934); *Rep. Prog. Phys.* **12**, 185 (1949); *Weld. J. (Miami)* **34**, 157 (1955).
- ²⁵F. Milstein, *J. Mater. Sci.* **15**, 1071 (1980).
- ²⁶F. Milstein and K. Huang, *Phys. Rev. B* **18**, 2529 (1978).
- ²⁷F. Milstein, R. Hill, and K. Huang, *Phys. Rev. B* **21**, 4282 (1980).
- ²⁸F. Milstein and B. Farber, *Phys. Rev. Lett.* **44**, 277 (1980).
- ²⁹P. Hohenberg and W. Kohn, *Phys. Rev.* **136**, B864 (1964); W. Kohn and L. J. Sham, *ibid.* **140**, A1133 (1965).
- ³⁰M. Born, *Proc. Cambridge Philos. Soc.* **36**, 160 (1940); M. Born and K. Huang, *Dynamical Theory of Crystal Lattices* (Clarendon, Oxford, 1956).
- ³¹R. Hill, *Math. Proc. Camb. Philos. Soc.* **77**, 225 (1975).
- ³²R. Hill and F. Milstein, *Phys. Rev. B* **15**, 3087 (1977).
- ³³F. Milstein and R. Hill, *Phys. Rev. Lett.* **43**, 1411 (1979); *J. Mech. Phys. Solids* **25**, 457 (1977); **26**, 213 (1978); F. Milstein, in *Mechanics of Solids*, edited by H. K. Hopkins and M. J. Sewell (Pergamon, Oxford, 1982), p. 417.
- ³⁴W. X. Li and T. C. Wang, *J. Phys.: Condens. Matter* **10**, 9889 (1998).
- ³⁵N. Churcher, K. Kunc, and V. Heine, *J. Phys. C* **19**, 4413 (1986).
- ³⁶(a) C. Cheng, R. J. Needs, and V. Heine, *J. Phys. C* **21**, 1049 (1988); (b) J. J. A. Shaw and V. Heine, *J. Phys.: Condens. Matter* **2**, 4351 (1990); (c) C. Cheng, V. Heine, and L. Jones, *ibid.* **2**, 5097 (1990); (d) C. Cheng, V. Heine, and R. J. Needs, *ibid.* **2**, 5115 (1990).
- ³⁷W. R. L. Lambrecht, B. Segall, M. Methfessel, and M. van Schilfgaarde, *Phys. Rev. B* **44**, 3685 (1991).
- ³⁸K. B. Tolpygo, *Fiz. Tverd. Tela (Leningrad)* **2**, 2655 (1960) [*Sov. Phys. Solid State* **2**, 2367 (1961)].
- ³⁹J. Teroff, *Phys. Rev. B* **39**, 5566 (1989).
- ⁴⁰E. Pearson, T. Takai, T. Halicioglu, and W. A. Tiller, *J. Cryst. Growth* **70**, 33 (1984).
- ⁴¹M. Kohyama, S. Kose, M. Kinoshita, and R. Yamamoto, *J. Phys.: Condens. Matter* **2**, 7791 (1990).
- ⁴²J. A. Majewski and P. Vogl, *Phys. Rev. B* **35**, 9666 (1987).
- ⁴³M. Tang and S. Yip, *J. Appl. Phys.* **76**, 2719 (1994).
- ⁴⁴C. Truesdell and R. Toupin, *Handbuch der Physik*, edited by S. Flügge (Springer-Verlag, Berlin, 1960), Vol. III, Chap. 1, p. 226.
- ⁴⁵M. Bockstedte, A. Kley, J. Neugebauer, and M. Scheffler, *Comput. Phys. Commun.* **107**, 187 (1997).
- ⁴⁶D. R. Hamann, *Phys. Rev. B* **40**, 2980 (1989).
- ⁴⁷N. Troullier and J. L. Martins, *Phys. Rev. B* **43**, 1993 (1991).
- ⁴⁸M. Fuchs and M. Scheffler (unpublished).
- ⁴⁹X. Gonze, R. Stumpf, and M. Scheffler, *Phys. Rev. B* **44**, 8503 (1991).
- ⁵⁰J. Perdew and A. Zunger, *Phys. Rev. B* **23**, 5048 (1981).
- ⁵¹C. S. G. Cousins, *J. Phys. C* **11**, 4867 (1978); **11**, 4881 (1978).
- ⁵²J. F. Nye, *Physical Properties of Crystals* (Clarendon, Oxford, 1957), Chap. VIII.
- ⁵³*Numerical Data and Functional Relationships in Science and Technology*, edited by O. Madalung, Landolt-Bornstein, New Series, Group III, Vol. 17, Pt. a (Springer, Berlin, 1982), p. 49.
- ⁵⁴R. D. Carnahan, *J. Am. Ceram. Soc.* **51**, 223 (1968).

- ⁵⁵D. W. Feldman, J. H. Parker, Jr., J. W. Choyke, and L. Patrick, Phys. Rev. **173**, 787 (1968).
- ⁵⁶A. Reuss, Z. Angew. Math. Mech. **9**, 55 (1929).
- ⁵⁷W. Voigt, *Lehrbuch de Kristalphysik* (Teubner, Leipzig, 1928).
- ⁵⁸R. Hill, Proc. Phys. Soc. London, Sect. A **65**, 349 (1952).
- ⁵⁹L. Kleinman, Phys. Rev. **128**, 2614 (1962).
- ⁶⁰A. J. G. Op Het Veld and J. D. B. Veldkamp, Fibre Sci. Technol. **2**, 269 (1970).
- ⁶¹B. N. Oshcherin, Phys. Status Solidi A **34**, K181 (1976).
- ⁶²F. Milstein and K. Huang, Phys. Rev. B **19**, 2030 (1979).
- ⁶³W. A. Harrison, *Electronic Structure and the Properties of Solids* (Cambridge University Press, New York, 1975), p. 17.
- ⁶⁴A. R. Verma and P. Krishna, *Polymorphism and Polytypism in Crystals* (Wiley, New York, 1966), p. 103.